Romanian Reports in Physics, Vol. 64, Supplement, P. 1195–1206, 2012

Dedicated to Professor Ioan-Iovitz Popescu's 80th Anniversary

MAGNETIC PROPERTIES AND ELECTRONIC STRUCTURES OF SOME PSEUDOBINARY RARE-EARTH COMPOUNDS

E. BURZO

"Babes-Bolyai" University, Faculty of Physics, Cluj-Napoca 400084,
and Romanian Academy of Science, Cluj-Napoca Branch, Cluj-Napoca 400015, Romania,
E-mail: emil.burzo@phys.ubbcluj.ro

Received July 18, 2012

Abstract. Band structure calculations and magnetic measurements were performed on $RNi_{5-x}Al_x$ and $RCo_{5-x}Si_x$ heavy rare-earth compounds with x = 0 and 1.0. The spin fluctuation system $LaNi_{5-x}Al_x$ was also analysed. The exchange interactions in magnetic ordered compounds were analysed in 4f-5d-3d model. The evolution with composition of the nickel and cobalt moments at 2c and 3g sites is discussed. The R5d band polarizations show linear dependences as function of De Gennes factor, G, with a slope $\alpha = 1.4 \cdot 10^{-2} \mu_B/G$. The different contributions to R5d band polarizations are analysed. The computed magnetic moments per formula unit agree with experimental data. The effect of pressure, as result of volume change, in $YCo_{5-x}M_x$ with M= Co, B and Si compounds are shortly presented.

Key words: rare-earth transition metal compounds, band structures, magnetic properties.

1. INTRODUCTION

The rare-earth and yttrium (R)-transition metal (M) compounds form an interesting group of magnetic materials having technical application [1]. The 4f electrons of rare-earths have a small spatial extent and consequently they are well localized. The 3d electrons of transition metals show a large range of magnetic behaviours. As function of crystal structure and composition, these cover the situation in which M atoms have well defined magnetic moments or are in non-magnetic state, crossing the region of onset/collapse of ordered moment. As example, cobalt in RCo_5 type compounds, has a well localized moment, while nickel in RNi_5 shows an itinerant magnetism. The YNi_5 or $LaNi_5$, at low temperatures, are exchange enhanced paramagnets.

The exchange interactions in magnetic ordered R-M compounds can be described by the phenomenological model proposed by Campbell [2]. In this model the 4f electrons of rare-earths polarize their 5d band. There are also short-range

R5d-M3d exchange interactions. In heavy rare-earth compounds the 4f moments and R5d band polarizations are parallely oriented, while transition metal moments couple antiparallely to the rare-earth ones. The R5d band polarizations, induced by 4f moments, are proportional to De Gennes factor [3]. There is also a contribution thought 4f-3d hybridization, proportional to the number of M atoms situated in the first coordination shell to R one as well as their moments.

The magnetic properties of some $RCo_{5-x}Si_x$ [4–6] and $RNi_{5-x}Al_x$ [7–17] were previously reported. It was shown that nickel in $RNi_{5-x}Al_x$ compounds has a very small moment or show a paramagnetic behavior, while the cobalt evidence a more localized behavior.

In order to obtain additional information on the magnetic behavior of Co and Ni in R-M type compounds we studied the $RCo_{5-x}Si_x$ and $LaNi_{5-x}Al_x$ systems with $x = 0$ and 1. These compounds crystallize in hexagonal $CaCu_5$-type structure. In this lattice the R atoms are located in 1a site, while M = Co and Ni occupy 3g and 2c type positions – Fig. 1.

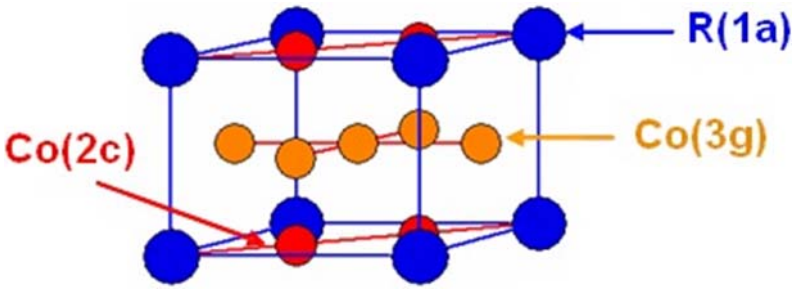

Fig. 1 – $CaCu_5$-type structure.

In addition to magnetic measurements, band structure calculations were performed. The evolution with composition of the Co and Ni moments in $CaCu_5$-type structure, both at 3g and 2c sites as well as the R5d band polarizations are analysed. The effect of pressure on the change of magnetic moments in YCo_4M (M = Co, B, Si compounds) were also discussed.

2. EXPERIMENTAL AND COMPUTING METHOD

The $RCo_{5-x}Si_x$ and $RNi_{5-x}Al_x$ compounds with $x = 0$ and 1.0 were prepared by arc melting in an induction furnace. The samples, were thermally treated at 900–1000^{o}C, in vacuum, for one week. The X-ray diffraction patterns evidenced the presence of only one phase. The compounds crystallize in $CaCu_5$-type structure.

The magnetic measurements were performed in the temperature range 1.7–300 K, and fields up to 90 kOe. In the paramagnetic range, the susceptibilities

were determined from their field dependences according to Honda-Arrott plot: $\chi_m = \chi + cM_sH^{-1}$, by extrapolating the measured values, χ_M, to $H^{-1} \rightarrow 0$ [18]. By c is denoted the impurity content and M_s is their saturation magnetization. By this method any possible alteration of magnetic susceptibilities, as a result of the presence of magnetic ordered phase, is avoided.

The ground state electronic structures and magnetic properties of the compounds have been studied by tight-binding linear muffin tin orbital method (TB-LMTO) within the atomic sphere approximation (ASA), together with the coherent potential approximation (CPA) [19]. The local spin density approximation (LSDA) was used for the exchange-correlation potential within Vosko-Vilk-Nussair parameterization [20]. All calculations have been performed using a mesh of 16×16×16 k-points in the full Brillouin zone (BZ) resulting in 274 k-points in the irreductible wedge of BZ.

The LSDA+U approximation was also used to compute the band structures for some compounds. The intra-atomic Coulomb interaction, U, was added [21]. As example, for Gd, the average Coulomb interaction U_f = 9 eV and exchange intraction J_J = 1 eV were chosen. For cobalt, U_d = 2 eV and J_d = 1 eV which are widely accepted values [3, 21, 22] were used.

The Al and Si atoms were considered to substitute Ni and Co, respectively at 3g sites, as previously showed [13].

3. MAGNETIC PROPERTIES

3.1. PARAMAGNETIC COMPOUNDS

The magnetic behavior of the exchange enhanced paramagnets $LaNi_{5-x}Al_x$ with x = 0 and 1.0 have been analysed [10]. The thermal variations of the reciprocal susceptibilities, for the above compounds, are plotted in Fig. 2. The magnetic susceptibilities increase up to temperatures located at T_m = 90 K (x = 0) and T_m = 12 K (x = 1.0), respectively. At higher temperatures, the magnetic susceptibilities can be described as a superposition of the Pauli paramagnetic term, χ_0, on a Curie-Weiss contribution:

$$\chi = \chi_0 + C(T - \theta)^{-1}. \quad (1)$$

By C is denoted the Curie constant and θ is the paramagnetic Curie temperature. The θ values are negative, as expected for a typical spin fluctuation system [23].

The effective nickel moments decrease from 2.15 μ_B/atom (x = 0) to 0.72 μ_B/atom (x = 1.0). These values are smaller than that expected for Ni^{2+} ion, namely M_{eff} = 2.83 μ_B.

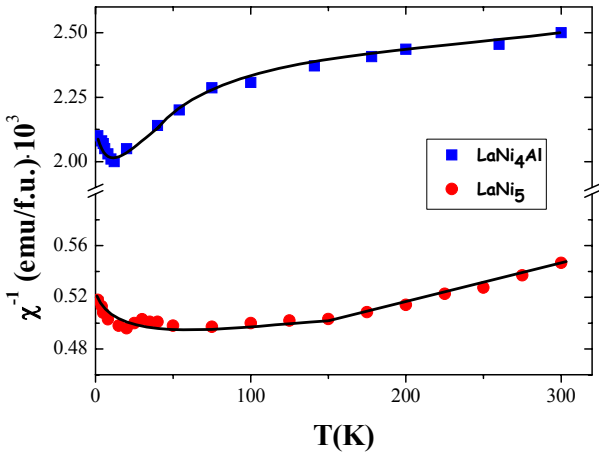

Fig. 2 – Thermal variations of reciprocal susceptibilities for $LaNi_5$ and $LaNi_4Al$.

In the temperature range, $T \leq 10$ K, the magnetic susceptibilities follow a T^2 dependence (Fig. 3).

$$\chi = \chi(0)[1+aT^2], \tag{2}$$

with $a = 1.3 \cdot 10^{-3} K^{-2}$ ($x = 0$) and $0.23 \cdot 10^{-3} K^{-2}$ for $LaNi_4Al$ compound.

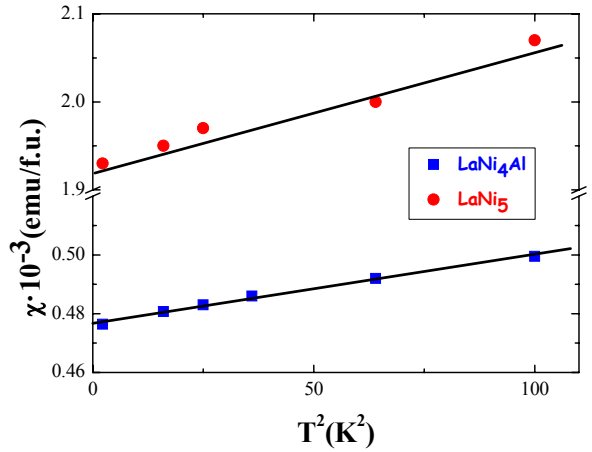

Fig. 3 – Thermal variations of magnetic susceptibilities, at $T \leq 10$ K, for $LaNi_5$ and $LaNi_4Al$.

The band structures of $LaNi_5$ and $LaNi_4Al$ are plotted in Fig. 4 together with XPS spectra. The Fermi levels, in $LaNi_5$ and $LaNi_4Al$ compounds, lie just above a large sharp peak in DOS, in a minimum of density of states. Alloying with Al induced changes in the Ni3d band. The density of states at the Fermi level is diminished as compared with that computed in $LaNi_5$. The maximum of the

valence bands is shifted to higher binding energy. The states at the Fermi level, in $LaNi_5$, have mainly d character. When alloying with aluminium, the s-p contribution to the DOS, at the Fermi level, increases. There is a diminution of d-electron correlations and the exchange enhancement factor decreases.

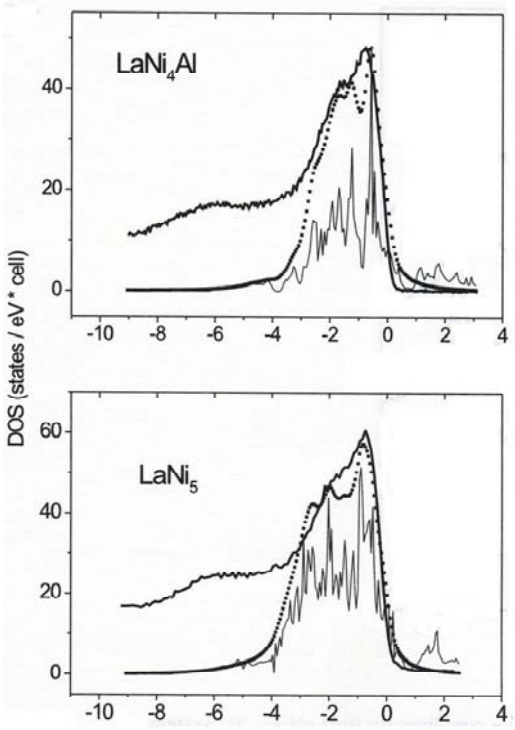

Fig. 4 – Comparison of measured XPS valence bands (thick solid curve), the calculated total DOS (solid curve) and the convoluted DOS (with Lorentzian of half-width 0.4 eV and taking into account appropriate cross-sections for partial bands with different l-symmetry, doted curve) for $LaNi_{5-x}Al_x$ with $x = 0$ and 1.0.

By using the calculated densities of states and taking into account the effect of spin fluctuations, the temperature dependences of the magnetic susceptibilities were analysed. In the low temperature range, by using the paramagnon picture [24], the coefficient a from relation (2) can be described by

$$a = \frac{\pi^2}{6}\left[2\frac{\eta''}{\eta} - 1.2\left(\frac{\eta'}{\eta}\right)^2\right]s^2, \tag{3}$$

where s is the exchange enhancement factor and by η, η' and η'' are denoted the density of states and their first and second derivatives, respectively.

A symmetric energy interval around the self-consistent value of the Fermi level was selected and a mean square interpolation scheme was used in order to evaluate the energy dependence of the density of states [12]. By using this approach, the first and second derivative of the DOS, at the Fermi level, were evaluated. The computed a values of $1.22 \cdot 10^3$ K^{-2} ($x = 0$) and $0.17 \cdot 10^{-3}$ K^{-2} ($x = 1$) are close to those experimentally determined.

In the high temperature range, $T \geq 100$ K, the contributions to the susceptibilities from the spin fluctuations, in terms of the computed density of states [25], were analysed. This method was already used to describe the temperature dependences of the magnetic susceptibilities in $YCo_{2-x}Ni_x$ compounds [26]. The temperature dependences of the mean square amplitudes of spin fluctuations $\langle S^2 \rangle$ were determined. There is a tendency to saturate the $\langle S^2 \rangle$ values at 300 K, but still remains somewhat smaller than the experimental ones.

3.2. MAGNETIC ORDERED COMPOUNDS

3.2.1. $RNi_{5-x}Al_x$ compounds

The band structure calculations were made on $RNi_{5-x}Al_x$ were R is a magnetic heavy rare-earth. As example in Fig. 5 are plotted the band structures for $TbNi_{5-x}Al_x$ with $x = 0$ and 1.0. The determined magnetic moments, in $TbNi_5$, when using LDA and LDA+U schemes are only little different. Values 0.25 (0.23) μ_B and 0.18 (0.15) μ_B were obtained for nickel magnetic moments at 3g and 2c sites by using LDA method. In parentheses are given the data obtained by LDA+U scheme.

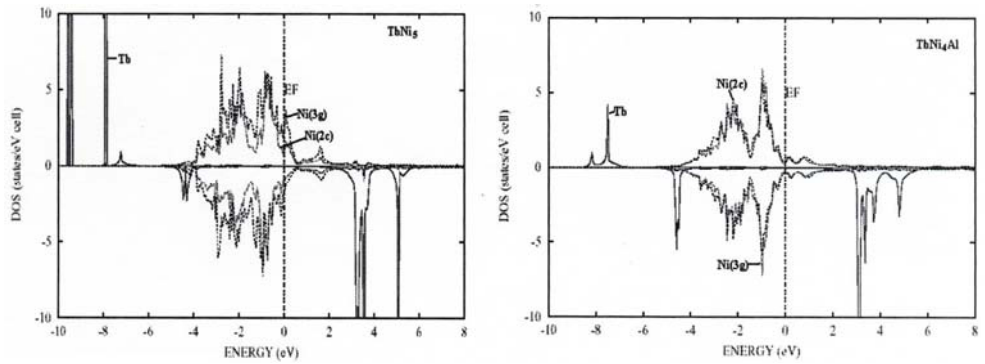

Fig. 5 – Band structures of $TbNi_{5-x}Al_x$ compounds with $x = 0$ and 1.0. The partial densities of states of Ni2c and Ni3g are also given.

The replacement of nonmagnetic La by a magnetic rare-earth induces through 4f-5d-3d interactions magnetic moments at both nickel sites. The number of Tb atoms in the first coordination shell to Ni3g is four and three for Ni2c. This can

explain the higher induced moments at 3g sites. When replacing Ni by Al, the nickel moments decrease both at 2c and 3g sites. Values $M_{Ni}(2c) = 0.02\ \mu_B$ and $M_{Ni}(3g) = 0.03\ \mu_B$ were obtained in case of $TbNi_4Al$ compound.

The composition dependences of the nickel moments at 2c and 3g sites, in RNi_5 and RNi_4Al heavy rare earth compounds, are plotted in Fig. 6, as function of De Gennes factor. Linear variations are shown with a slope of $1.4\cdot10^{-2}\ \mu_B/G$. The computed nickel moments in RNi_4Al are rather small and consequently the errors in their evaluation can be of the order of their magnitudes. The tendency to decrease the computed values, with decreasing De Gennes factor is evident.

The R5d band polarizations both in RNi_5 and RNi_4Al compounds show linear dependences as function of $G = (g_J–1)^2J(J+1)$ parameter – Fig. 7.

$$M_{5d}= M_d(0)+\alpha G, \tag{4}$$

with $\alpha=1\cdot10^{-2}\ \mu_B/G$.

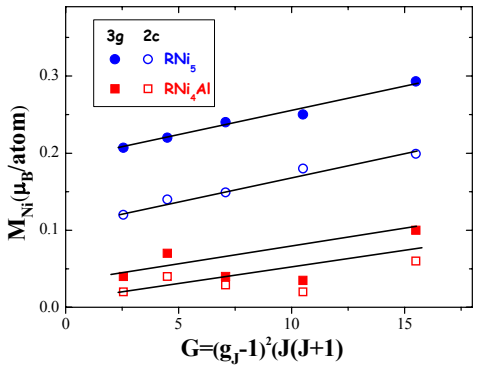

Fig. 6 – Computed magnetic moments at 3g and 2c sites in RNi_5 and RNi_4Al compounds.

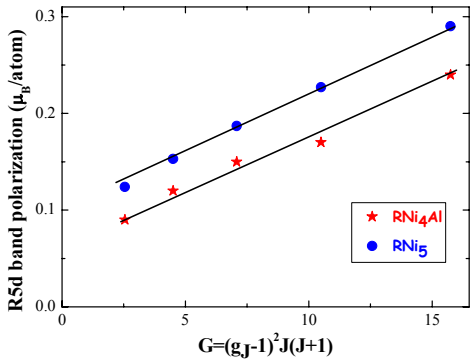

Fig. 7 – The R5d band polarizations in RNi_5 and RNi_4Al compounds.

The $M_{5d}(0)$ values, obtained by extrapolation at $G = 0$ are 0.09 μ_B ($x = 0$) and 0.05 μ_B ($x = 1$), respectively.

In case of $Gd_xLa_{1-x}Ni_5$ system there was shown, in addition 5d-3d interactions, also 5d-5d exchange interactions through 5d orbitals having lobes oriented along **c**-axis. Thus, at the $M_{5d}(0)$values, in addition to 5d-3d hybridizations effects, the contributions of 5d-5d exchange interactions may be also considered. This is in agreement with a smaller decrease of $M_{5d}(0)$ than expected due to diminution of Ni moments, as result of nickel substitution by aluminium.

When subtracting $M_{5d}(0)$ values from the M_{5d} ones, the contributions αG to R5d band polarizations, due to local 4f-5d interactions, can be obtained. For a given R atom, the same αG contributions can be obtained both in RNi_5 and RNi_4Al compounds. As example, values of $\cong 0.20\ \mu_B$ are obtained in gadolinium and 0.08 μ_B in dysprosium compounds.

The computed magnetic moments per formula unit are in rather good agreement with experimental values, as seen in Table 1. Since of the low Curie temperatures of $RNi_{5-x}Al_x$, with R = Dy,Ho, the accurate saturation magnetization is difficult to be obtained and extrapolation of the measured values from 4K to absolute temperature can lead to some errors. These can explain, at least partially, the differences between experimental and computed values.

Table 1

Magnetic moments

	Magnetic moment (μ_B/f.u.)							
	$GdNi_5$	$GdNi_4Al$	$TbNi_5$	$TbNi_4Al$	$DyNi_5$	$DyNi_5Al$	$HoNi_5$	$HoNi_4Al$
Experimental	6.10	6.80	8.25	8.10	9.31	9.10	8.70	8.80
Computed	6.00	6.80	8.20	8.95	9.10	9.90	9.15	9.80

3.2.2. $RCo_{5-x}Si_x$ compounds

The band structure of $GdCo_4Si$ compound, computed by using LDA+U method is given in Fig. 8. Similar patterns were observed both using LDA or LDA+U schemes for all heavy rare earth or yttrium RCo_4Si compounds. The Fermi levels are situated in a peak of the density of states for Co spin up subbands, both at 3g and 2c sites. The corresponding densities of states for spin down subband is rather low. The band structures resemble with those of RCo_5 compounds. The computed magnetic moments at 3g and 2c sites are shown in Fig. 9a while in Fig. 9b are given the R5d (Y4d) band polarizations as function of De Gennes factor. The R5d(Y4d) values for RCo_5 compounds are also given.

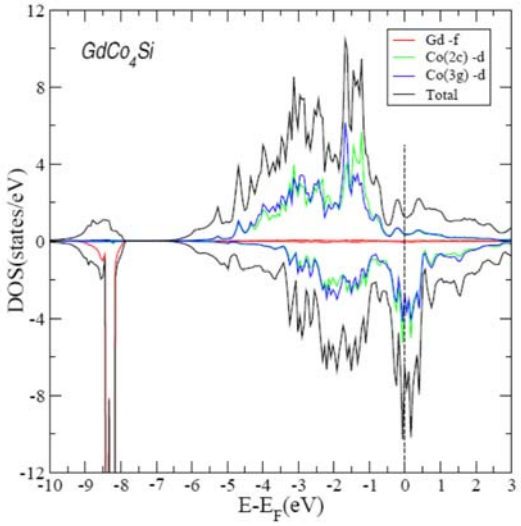

Fig. 8 – Band structure of $GdCo_4Si$ compound.

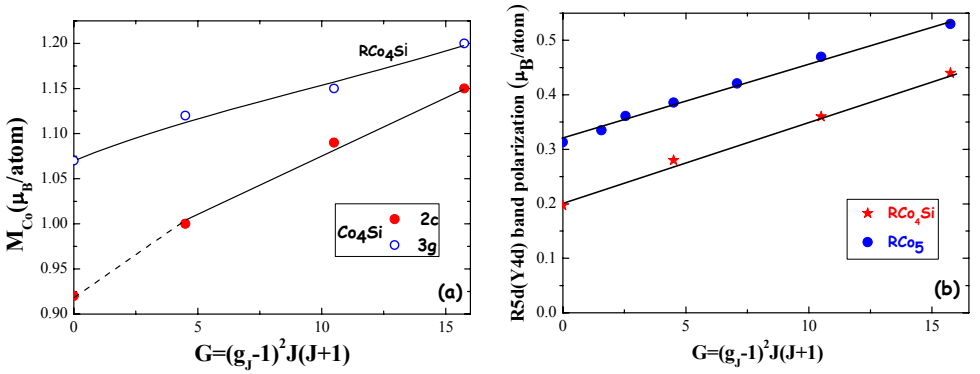

Fig. 9 – The dependences of cobalt moments in RCo_4Si (a) and of R5d band polarizations in $RCo_{5-x}Si_x$ compounds with $x = 0$ and 1.0 (b).

The cobalt moments vary in a smaller extent than nickel ones in $RNi_{5-x}Al_x$ compounds, showing a more localized behavior.

The R5d band polarizations are linearly dependent on De Gennes factor and described by the relation (4) with $\alpha \cong 1.4 \cdot 10^{-2}$ μ_B/G, the same as in $RNi_{5-x}Al_x$ compounds. The $M_{5d}(0)$ values are 0.32 μ_B ($x = 0$) and 0.21 μ_B ($x = 1$). The decrease of $M_{5d}(0)$ value when replacing Co by Si can be correlated with the decrease of cobalt moments. The αG values determined by local 4f-5d exchange are nearly the same as those determined in $RNi_{5-x}Al_x$ compounds. These data suggest that for a given type structure and R atom the induced band polarizations by local 4f-5d interactions are similar.

4. PRESSURE EFFECTS ON THE MAGNETIC BEHAVIOUR OF $YCo_{5-x}M_x$ (M=Co, B, Si) COMPOUNDS

The transition of cobalt moments in YCo_5 to a low spin state, under lattice contraction, was theoretically predicted [27]. No estimation of the threshold pressure was made. Latter on, was shown that YCo_5 loses its magnetic strength under hydrostatic pressure [28]. The density-functional calculations evidenced that the high hydrostatic pressure destroys the strong ferromagnetism of YCo_5 [29]. The transformation proceeds in a stepwise fashion as a first order transition, at $p = 18 \pm 2$ GPa and is accompanied by an isomorphic lattice collapse and a topological change, of the Fermi surface.

Band structure calculations were performed on YCo_4M with M = Co, B and Si, in order to analyse the effects of volume changes, reflecting the pressure effects on their magnetic behaviour. In all cases the c/a ratio was considered to be constant and of 0.81 for YCo_5. The evolution with relative volume of the cobalt moments at 2c and 3g sites in YCo_5 and YCo_4B are plotted in Fig. 10.

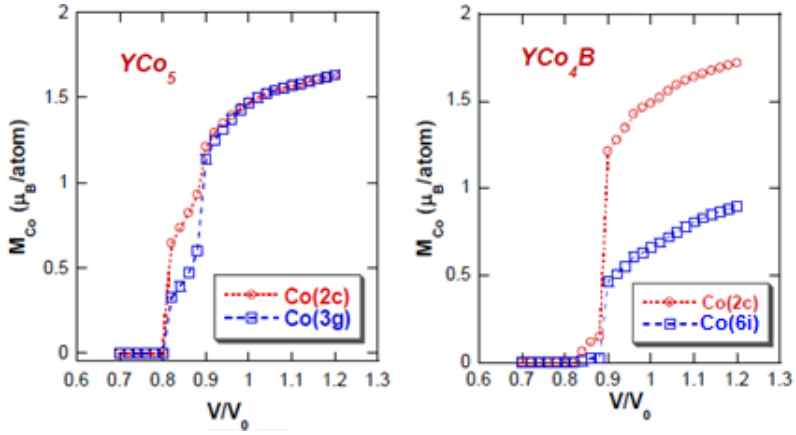

Fig. 10 – The dependeces of cobalt moments at 2c and 3g(6i) sites on the volume variations, reflecting the pressure effects in YCo_5 and YCo_4B compounds.

The dependences of the cobalt magnetic moments at 2c and 3g sites are somewhat different in YCo_5, when relative volume diminished. A sudden decrease of the cobalt magnetic moments at 3g sites was shown for v/v_o = 0.92, which correspond to a volume v = 74·1 Å^3. This volume is close to the critical value previously reported [29], where a sudden change of the cobalt moments was reported. A full collapse of the cobalt moments is suggested for a relative volume v/v_o = 0.81. Different behavior of cobalt moments at 2c and 3g sites, in the range $0.81 \leq v/v_o \leq 0.90$ is evidenced. These can be correlated with the different local environments of 2c and 3g sites in $CaCu_5$-type structure.

The evolution with relative volume of the cobalt moments at 2c and 6i sites in YCo_4B is somewhat different. We note that the crystal structure of YCo_4B is derived from $CaCu_5$-type by substituting Co2c by B atoms every second layer. A collapse of the cobalt moments at v/v_o = 0.91 was shown both at 2c and 6i sites. The collapse is directly to a nonmagnetic state for 3g sites and only up to $\cong 0.2\ \mu_B$ for cobalt at 2c site. For the later site, the nonmagnetic state is evidenced for $v/v_o \geq 0.84$.

In case of YCo_4Si, a sudden decrease of the magnetic moments at both 2c and 3g sites, up to 0.32 μ_B/atom is evidenced, at v/v_o=0.92, followed by a linear change at $v/v_o \leq 0.92$. The different behavior, as compared to YCo_5, can be correlated with an increase of the itinerancy degree of cobalt moments both in YCo_4B and YCo_4Si compounds.

5. DISCUSSIONS

The nickel moments in $RNi_{5-x}Al_x$, compounds with x = 0 and 1, show a typical spin fluctuation behavior [23]. In case of exchange enhanced paramagnets,

as $LaNi_{5-x}Al_x$, as function of temperature, there is a transition from a T^2 type dependence of the magnetic susceptibilities typical for a Pauli type paramagnet to a Curie-Weiss type behavior. This dependence is typical for a spin fluctuation system. The spin fluctuations seems to be nearly saturated at $T > 250$ K. The effective nickel moments are smaller than those of Ni^{2+} ions. This behavior can be correlated with hybridization effects, particularly in $LaNi_4Al$ compound.

In magnetic heavy rare earth compounds, RNi_5, the Ni moments at 2c and 3g sites are induced through 4f-5d-3d type interactions. The nickel moments are proportional to De Gennes factor as expected in the above model. In RNi_4Al compounds as result of the hybridization with aluminium p states, the nickel moments are strongly decreased.

A diminution of cobalt moments in RCo_4Si, as compared to RCo_5 is shown. The degree of itinerancy as evidence by the ratio, r, between the number of spins determined from Curie constants and saturation magnetizations is situated in the range $2.0 \leq n \leq 3.2$. Also, the r values follow a $T_c^{-2/3}$ dependence [6] as expected in spin fluctuation model.

The R5d band polarization are linearly dependent on the De Gennes factor, having identical slopes in all the studied compounds having $CaCu_5$-type structure. Thus, the αG contribution to the R5d band polarization is the same for a given rare-earth. The variable contributions to R5d band polarizations for a given R are due to contributions both from 5d-3d and 5d-5d interactions.

The computed magnetic moments per formula unit agree with experimental values.

The cobalt magnetic moments in $YCo_{5-x}M_x$ (M = Co, Si, B) are sensitive to volume reduction, pressure effect, respectively. Preliminary study evidenced somewhat different behavior of cobalt at 2c and 3g sites in YCo_5 compound. As result of the substitutions and increasing delocalization of cobalt moments, their collapse in YCo_4M compounds takes place at smaller volume variations, than evidenced in YCo_5.

REFERENCES

1. E. Burzo, A. Chelkowski and H.R. Kirchmayr, *Landolt Börnstein Handbook*, Springer Verlag, Vol. **III/19d2** (1990).
2. J. Campbell, J. Phys. F.: Metal Phys., **2**, L47 (1972).
3. E. Burzo, L. Chioncel, R. Tetean and O. Isnard, J. Phys.: Condens. Matter, **23**, 026001 (2011); E. Burzo, Rom. J. Phys., **57**, 82 (2012).
4. C.V. Thang, L.H. Nam, N.P. Dong, N.P. Thuy and E. Bruck, J. Magn. Magn. Mater., **196,** 765 (1999).
5. N. Coroian, K. Klosek and O. Isnard, J. Alloys Comp., **427**, 5 (2007).
6. E. Burzo, P. Vlaic and I. Creanga, J. Alloys Comp., **509**, 8289 (2011); E. Burzo, V. Pop, C.D. Buda and I. Costina, Balkan Phys. Lett., **5**, 1247 (1997).
7. T. Tolinski: Modern Phys. Letters, B**21**, 431 (2007).

8. T. Tolinski, A. Szewczyk, M. Gutowska, A. Kowalczyk: Phys. Stat. Solidi (b), **242**, R42 (2005).
9. Y.V. Knyazev, A.V. Lukoyanov, Y.I. Kuzmin and A.G. Kuchin, Phys. Stat.Solidi (b), **249**, 824 (2012).
10. E. Burzo, S.G. Chiuzbaian, M. Neumann and L. Chioncel, J Phys.: Condens. Matter, **14**, 8057 (2002).
11. E. Burzo, A. Takacs, M. Neumann and L. Chioncel, Phys. Stat Solidi (c), **1**, 3343 (2004);
E. Burzo, C. Pacurar and I. Balasz, Mol. Cryst. Liquid Cryst., **415**, 117 (2004).
12. E. Burzo, S. Chiuzbaian, L. Chioncel and M. Neumann, J. Phys.: Condens. Matter, **12**, 5897 (2000).
13. E. Burzo, S. Chiuzbaian, M. Neumann, L. Chioncel, M. Valeanu and I. Creanga, J. Appl. Phys., **92**, 7362 (2002).
14. E. Burzo, L. Chioncel, I. Costina and S.G. Chiuzbaian, J. Phys.: Condens. Matter, **18**, 4861 (2006).
15. Z. Blazina, S. Sorgic and A. Brasner, J. Phys.: Condens. Matter, **11**, 3105 (1999).
16. G. Chelkowska, A. Bajorek, A. Katolik and L. Sliwinski, J. Magn. Magn. Matter., **e455**, 272–276 (2004).
17. M. Coldea, S.G. Chiuzbaian, M. Neumann, D. Todoran, M. Demeter, R. Tetean and V. Pop, Acta Phys. Polonica, **A98**, 629 (2000).
18. L.F. Bates, *Modern Magnetism*, Cambridge University Press, UK, 1951, p.133.
19. I. Turek, V. Drchal, J. Kudronovsky, M. Sob and P. Weinberger, *Electronic Structure of Disordered Alloys, Surfaces and Interfaces*, Kluwer Academic, Boston, 1997.
20. S.H. Vasko, L. Wilk and M. Nussair, Canad. J. Phys., **58**, 1200 (1980).
21. V.I. Anisimov, F. Argasetiavan and A.I. Lichtenstein, J. Phys.: Condens. Matter, **9**, 767 (1997).
22. I. Yang, S.V. Savrasov and G. Kotliar, Phys. Rev. Lett., **87**, 216405 (2001).
23. T. Moriya, J. Magn. Magn. Mater., **100,** 201 (1991).
24. M.T. Beal-Monod and J.M. Lawrence, Phys. Rev., **B21**, 5400 (1980).
25. M. Shimizu, Rep. Progr. Phys. **44**, 21 (1981); Phys. Letters, **81A**, 87 (1981).
26. L. Chioncel, E. Burzo, R. Tetean and V. Pop, Mol. Cryst. Liquid Cryst., **417**, 513 (2004).
27. H. Yamada, K. Terao, F. Ishikawa, M. Yamaguchi, H. Mitamura and T. Goto, J. Phys.: Cond. Matter, **11**, 483 (1999).
28. H. Rosner, D. Koudela, U. Schwarz, A. Handstein, M. Hanfland, I. Opahle, K. Koepernik, M.D. Kuzmin, K.H. Muller, J.A. Mydosh, M. Richter, Nature, Phys., **2**, 469 (2006).
29. D. Koudela, U. Schwarz, H. Rosner, U. Burkhardt, A. Handstein, M. Hanfland, M.D. Kuzmin, I. Ophale, K. Kopernik, K.H. Müller, M. Richter, Phys. Rev., **B77**, 024411 (2008).